Computational Model of Large Capacity Molten Sulfur Combustion Spray Efficacy and Process Efficiency

Kathleen J. Brown*, Kyle Bade, and Rudi J. Schick
Spray Analysis and Research Services
Spraying System Company
P.O. Box 7900
Wheaton, IL 60187 USA

Abstract
The use of precision spray injectors with advanced technology nozzles in the combustion of molten sulfur represents an active and growing field. The efficient combustion of large molten sulfur volumes is a clear requirement in the phosphate creation industry. Spraying Systems Company, along with our industry partners, have conducted significant research both the laboratory as well as in full scale industrial setting to arrive at optimized process solutions for this application. Additionally, Computational Models have been developed to allow for the assessment and optimization of the sulfur combustion efficacy. This paper presents the results of a detailed spray injection modeling study demonstrating the scale up of the spray solution as well as the 100% spray combustion requirement at these elevated sulfur flow capacities. Through the use of the models developed here, the sulfur combustion was improved beyond that which was possible using experimental results.

Introduction

Background

Sulfur trioxide (SO_3) is commonly used in the manufacturing of sulfuric acid, oleum, chlorosulfonic acid and other compounds. One method of attaining SO_3 gas for these processes is through the combustion of molten sulfur.

The sulfur is liquefied and fed into the combustion chamber of a furnace through one or injectors. These precision spray injectors are a critical component in the process. The injectors convert large quantities of molten sulfur into an atomized spray of sulfur particles. Control of the particle size is a critical factor in ensuring rapid vaporization and complete combustion within the combustion chamber. Unburned sulfur can deposit outside of the combustion zone which results in process inefficiency and increased maintenance.

This work outlines the design considerations for a successful sulfur combustion injection system. The process details injector selection and empirical characterization of the injector. Additionally the injection system design is evaluated via computational fluid dynamics (CFD) to ensure intended performance characteristics in the combustion chamber. These simulations address velocity profiles, temperature profiles, droplet tracking (devolitization), and other relevant characteristics of the application.

Theoretical Considerations

Atomization

The process of atomization is used in many spray applications to produce high surface area to volume ratios of the generated droplets. Often this high ratio provides much more efficient use of the spray droplets in evaporative and/or combustion processes. In general, atomizers which cause the greatest physical interaction between the liquid and vapor are most effective.

Liquid Jet Atomization

The atomization of any liquid jet into a gas region can be characterized into primary and secondary mechanisms. Primary atomization is caused by the initial instabilities within the liquid jet which act to disintegrate the jet internally. Secondary atomization considers the further breakup of drops larger than the critical drop size. In characterizing a jet there are two main properties which are often discussed: the continuous jet length and the drop size which may be used to evaluate the expected breakup of a jet.

Jet Breakup

A liquid jet exhausted into air may do so in a laminar or turbulent state. A laminar jet, which contains fluid particles which are traveling in parallel at the exit plane, may be created by utilizing a rounded inlet, having no mid-flow disturbances, and using a high viscosity liquid. Turbulence in jets, which aides in jet breakup, may be encouraged through high flow velocities, large tube sizes, general surface roughness, rapid cross-sectional changes, and perturbations due to flow obstructions or vibrations. The Reynolds number, $Re = \rho_L U_R D / \mu_L$, which relates pressure and viscous forces, may be used to determine the likelihood of a flow to be laminar (low Re number) or turbulent (high Re number). The critical Reynolds number identifies where laminar flow will undergo the transition to turbulent flow. For pipe flow, the critical Reynolds number is $Re_{crit} \approx 2300$. When a flow transitions from laminar to turbulent flow, the mechanisms governing jet breakup change and cause a decrease in jet breakup length.

Liquid Sheet Breakup

Fraser & Eisenklam (1953) defined and described three liquid sheet breakup regimes: Rim, Perforated Sheet, and Wave. Liquid surface tension and viscosity are the primary properties which determine which mode(s) of disintegration occur.

Liquid sheet breakup through "rim" disintegration often occurs with a high viscosity, high surface tension type liquids. In rim disintegration the liquid mass becomes thicker at the free edges which ultimately form liquid threads which breakup into large drops, whereas the internal area disintegrates and forms smaller drops.

In a "perforated sheet" type breakup, many holes are developed in the liquid sheet. The edges of these holes become thicker as the holes grow and more fluid mass is combined at each hole-edge. These holes continued to grow until they encounter other rims and coalesce. Many size drops are created.

"Wave" disintegration occurs when wave motions within the liquid sheet cause fluctuations with distinct wavelengths. These waves break-up into whole or half wavelength sections and surface tension reforms the sections into strands. These strands then disintegrate into drops. Wave disintegration creates drops that vary the most in size.

Drop Breakup

Atomization is the process by which a liquid jet is disintegrated by aerodynamic forces. These aerodynamic forces which cause the liquid to form into small drops, and often further breakdown into droplets, are created by the relative velocities of the liquid jet to its surroundings. The breakdown of drops in a spray can be summarized with an internal/external force assessment. The external aerodynamic pressure is balanced by the surface tension in order for the internal drop pressure to remain at a constant level, which it must in order to sustain its drop-size. In the event that the external forces are too large to be balanced though an increase in effective surface tension, the surface tension will be drastically increased through a decrease in the diameter

of the drop (drop splitting). The process of drop splitting takes place until the surface tension pressure is large enough to counteract the aerodynamic drag pressure at all points on the drop's surface. The drop size at this equilibrium level is known as the critical drop size. The mechanisms which cause the breakup of drops can be further identified by considering some of the more complex aspects of 'real world' conditions.

In turbulent flow fields the relative velocity between a drop and the surrounding gas will be very high, either locally or on a global scale. The turbulent field will impart a dynamic force on the drop which will determine the largest drop size that may exist in equilibrium due to the energy in the most disruptive turbulence scales (E). With dynamic turbulent forces present, the Weber number, $We = \rho_A U_R^2 (D/\sigma)$, which for low-viscosity liquids relates the *deforming* external pressure forces to the *reforming* surface tension forces of a liquid drop in air, can be evaluated for low-viscosity liquids and used to estimate the maximum drop s based on these scales.

In high viscosity (low Reynolds number) flow fields, where dynamic forces no longer control breakup, the surface tension forces and viscous forces work to deform and reform liquid drops. It is generally very difficult to atomize liquids that have a high viscosity ratio of the liquid to air. In these high-viscosity flows, variations in the air viscosity make little difference on the atomization process. Also, high-viscosity liquid phase spray material delays the breakup of drops and impedes atomization which is why more aggressive methods, such as air-blast atomization, are often used.

IN PRACTICE
Hydraulic Nozzles
Hydraulic nozzles are pressure driven nozzles which spray a single fluid. Many different types of hydraulic nozzle designs exist which aim to accomplish a variety of spray objectives from a continuous stream to a dispersed spray. These nozzles rely solely upon high liquid-to-gas relative velocities at exhaustion to achieve atomization. Liquids with low viscosity/high velocities more readily atomize; therefore hydraulic nozzles may suffice.

Two-Fluid (Pneumatic) Nozzles
The mixing of two fluids (usually one liquid phase and one gaseous phase) by a nozzle may be accomplished either internally or externally to the nozzle body. In an internally mixing nozzle, the liquid flow and gas flow interact upstream of the final discharge orifice. In this case, the mixture exits as a single, mixed flow; which widens with a reduced liquid flow velocity due to the pressurized gas. An internally mixing nozzle is optimum for high-viscosity fluids in a low flow rate application since the breakup of this type of flow is more difficult. However, the flow rate of each fluid is then coupled and to reach a desired operating condition, both flow rates must be tuned.

In an externally mixing nozzle the two fluid flows do not interact until after exiting the final nozzle orifice. These nozzle types may be designed to generate varies spray characteristics depending on the atomizing air pressure. However, due to the un-coupling of the two fluid streams, these nozzles are much less efficient in their use of the atomizer fluid. Also, externally mixing nozzles do not offer the possibility of the liquid flow to 'backup' into the gas flow orifice; this may be a benefit in certain processes.

Fluid Considerations
The spray angle of a nozzle represents the expected coverage of a spray after exiting from a nozzle. The theoretical spray angle (the angle in the near exit region) will diminish at larger downstream distances. Higher viscosity liquids will tend to form less divergent sprays whereas lower viscosity liquid sprays more easily disperse into a wide spray. The surface tension of the spraying liquid has a direct effect on the spray angle. Liquids with lower surface tensions form wider sprays.

The liquid properties such as (dynamic) viscosity, density, and surface tension directly effect and determine the spray type and quality which is created at a given operating condition. Liquid viscosity is representative of the willingness of a fluid to take the shape of its surroundings. A high viscosity fluid (syrup-like) will resist conforming to its surroundings and will move very slowly. The liquid viscosity directly affects the pattern at which a liquid will spray. High viscosity liquids require a higher pressure to spray due to their resistance to flow and will naturally form narrower sprays. Liquid density is directly proportional to the capacity of a spray. Density represents the mass-to-volume ratio for a liquid and therefore spraying a high-density liquid at a given velocity will result in a higher capacity spray. Liquid surface tension is a property representative of the internal force which holds a liquid together. This internal tension affects the liquid sprays minimum operating pressure, spray angle, and drop size. A higher surface tension will require a higher operating pressure, reduce the spray angle, and produce larger drop sizes.

Molten sulfur is highly influenced by temperature and thus temperature of the liquid feed through the injector is required to be tightly controlled. This is achieved by means of steam jacketed lining. Steam must be continually circulated to maintain the expected physical properties of the molten sulfur and corresponding spray performance. See Table 1 [6] for representative liquid properties and their general affects. Figures 1a and 1b [7] detail the temperature dependent nature of sulfur density and viscosity.
Table 1.

Atomization & Fluid Properties

| Fluid Property	Increase in Operating Pressure	Increase in Specific Gravity	Increase in Viscosity	Increase in Liquid Temperature	Increase in Surface Tension
Pattern Quality	Improves	Negligible	Worsens	Improves	Negligible
Capacity	Increases	Decreases	Nozzle Dependent	Fluid and Nozzle Dependent	No Effect
Spray Angle	Increases/ Decreases	Negligible	Decreases	Increases	Decreases
Drop Size	Decreases	Negligible	Increases	Decreases	Increases
Velocity	Increases	Decreases	Decreases	Increases	Negligible
Impact	Increases	Negligible	Decreases	Increases	Negligible
Wear	Increases	Negligible	Decreases	Fluid and Nozzle Dependent	No Effect
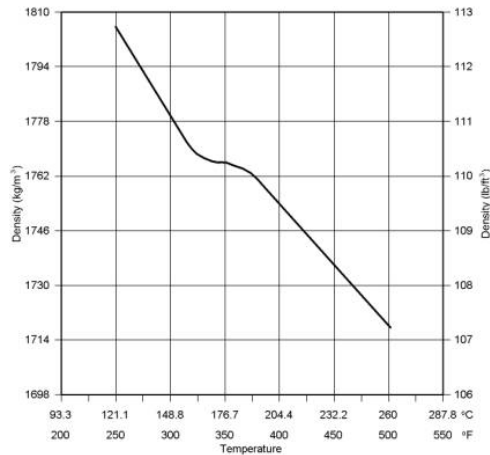
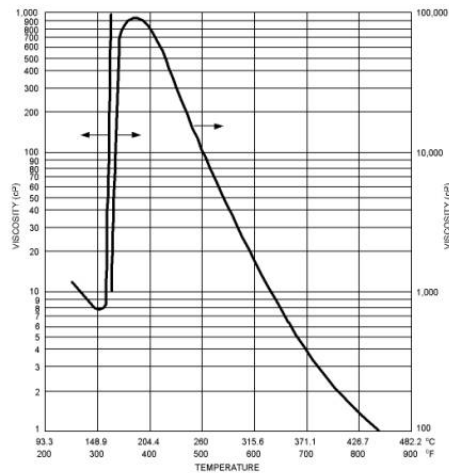Figure 2a. **Sulfur Density with respect to Temperature**

Figure 1b. **Sulfur Viscosity with respect to Temperature**

Injector Property Considerations

Nozzle construction materials may vary from light weight plastics to case hardened metals. The material which is most suited to an application directly depends on the spray substance, spray environment (corrosive, heated, etc.), and desired spray characteristics.

Typical furnace temperatures are in the range of 900°C - 1500°C. In order to function properly the injector must withstand the external temperatures, inter-nal temperatures, exposure to process fluids and internal forces. There are many readily available heat-resistant injector materials such as 310SS, 304SS, 316SS or 309SS or similar materials; the combination of material and design must be evaluated and optimized for each application.

Injector Design

Spraying Systems Co. patented (PAT# 6,098,896) design of an "Enhanced Efficiency Nozzle for use in Fluidized Catalytic Cracking" provides a refined solution to the FCC feed injection process. The use of an impingement pin, along with a transversely intersecting steam flow, greatly improves the efficacy and efficiency of the FCC feed injection process. In addition to these elements, the patented FCC unit provides specification for exit nozzle configurations to improve the post-discharge atomization of the fluid. Figure 1 provides a schematic representation of one of the Spraying Systems Co. FCC unit design configurations.
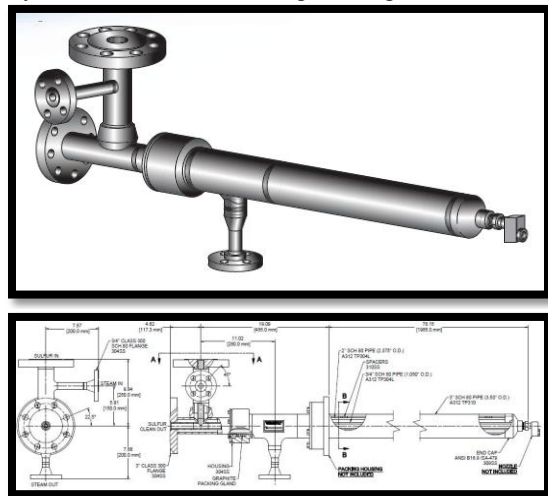

Figure 2. **Patented Sulfur-Burning Injector 53686-001 with 1/2BA-309SS70 Nozzle**

Through the results presented in the patent, the major design aspects (specifically the dual exit orifice) implemented in the unit are shown to improve the operation of the FCC injection process. The Spraying Systems Co. FCC nozzle offers many advantages, some of which are:

- Flat Spray pattern to fit exact coverage with maximum atomization for a given amount of steam or flow
- Controlled spray velocity
- Each injector nozzle is custom designed to exact specifications to maximize performance

- Ability to provide good atomization at relatively low ΔP (30-40 psi liquid; 50-60 psi stream)
- Large non-clogging passages
- Rugged, durable construction
- On-going research for improved product
- Products are design patent protected 25 years of continuous service

This FCC nozzle design was fabricated and experimentally tested under conditions outlined in the following sections.

These experimental tests, aimed at better understanding the atomization process/system presented by this nozzle, were conducted using a one-eighth scale model nozzle. These tests were conducted using a 2" CS FCC feed, single slot orifice injector nozzle, which was modeled after a commercial unit. The production size unit's liquid inlet flange-to-exit orifice OAL centerline distance is 54". The results of these tests help to characterize the spray created by this nozzle. The numerical simulation conducted for this work helps to characterize the internal mechanisms which could not be investigated experimentally. These results provide a better understanding of the output of this nozzle and the mechanisms which allow it to perform as it does.

EXPERIMENTAL TESTING

Test Setup and Data Acquisition

For drop sizing, the nozzle was mounted on a fixed platform 72" from the floor. A fixed assembly held the nozzle in place and data were acquired at 36" downstream of the nozzle exit. Drop size and velocity data was collected at various operating conditions.

A two-dimensional Artium Technologies PDI-200MD [6, 7, 8, 9] system was used to acquire drop size and velocity measurements. The solid state laser systems (green 532 nm and red 660 nm) used in the PDI-200MD are Class 3B lasers and provide 50-60mWatts of power per beam. The lasers were operated at an adequate power setting to overcome interference due to spray density.

The transmitter and receiver were mounted on a rail assembly with rotary plates; a 40° forward scatter collection angle was used. For this particular test, the choice of lenses was 1000mm for the transmitter and 1000mm for the receiver unit. This resulted in an ideal size range of about 4.0μm – 1638μm diameter drops. The optical setup was used to ensure acquisition of the full range of drop sizes, while maintaining good measurement resolution. The particular range used for these tests was determined by a preliminary test-run where the $D_{V0.5}$ and the overall droplet distribution were examined. For each test point, a total of 10,000 samples were acquired. The experimental setup can be seen in Figures 3a and 3b.
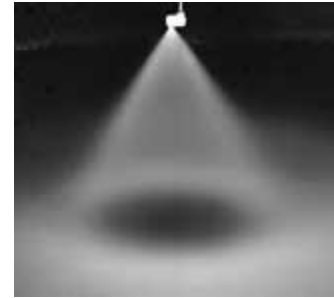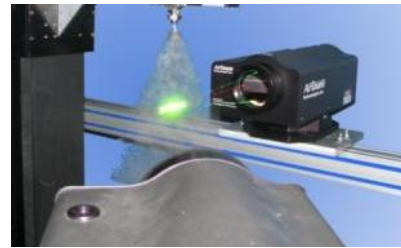

Figure 3a **- BA WhirlJet Nozzle Spray**

Figure 3b **- PDI Testing Setup**

The DV0.1, DV0.5, D32, and DV0.9 diameters were used to evaluate the drop size data. This drop size terminology is as follows:

DV0.1: is a value where 10% of the total volume (or mass) of liquid sprayed is made up of drops with diameters smaller or equal to this value.

D32: Sauter Mean Diameter (also known as SMD) is a means of expressing the fineness of a spray in terms of the surface area produced by the spray. SMD is the diameter of a drop having the same volume to surface area ratio as the total volume of all the drops to the total surface area of all the drops.

DV0.5: Volume Median Diameter (also known as VMD or MVD). A means of expressing drop size in terms of the volume of liquid sprayed. The VMD is a value where 50% of the total volume (or mass) of liquid sprayed is made up of drops with diameters equal to or smaller than the median value. This diameter is used to compare the change in average drop size between test conditions.

DV0.9: is a value where 90% of the total volume (or mass) of liquid sprayed is made up of drops with diameters smaller or equal to this value.

By analyzing drop size based on these standardized drop statistics it is possible to objectively characterize the quality and effectiveness of this atomizing nozzle for the prescribed application.

Test Fluids and Monitoring Equipment

All testing was conducted using water. Liquid flow to the system was supplied using a high volume pump at full capacity. The liquid flow rate to the atomizer was monitored with a MicroMotion D6 flow meter and controlled with a large bleed-off valve. The MicroMotion flow meter is a Coriolis Mass flow meter which measures the density of the fluid to determine the volume flow. The meter is accurate to ±0.4% of reading. Lliquid pressures were monitored upstream of the nozzle with 0-1.73MPa, class 3A pressure gauges. Pictures of the setup and operation of the test nozzle were provided in Figures 2a and 2b.

Test Conditions

Data were acquired for a total of 5 test cases. These tests involved the interaction of various liquid pressure levels and flow rates for five nozzle capacities. Figure 5 provides a detailed list of these test conditions. The testing was carried out at these operating conditions in order to characterize the nozzle's spray at various testing conditions and determine optimal operating conditions for this application.

NUMERICAL SIMULATIONS
CFD Methods

Computational Fluid Dynamics (CFD) is a numerical method used to numerically solve fluid flow problems. Today's CFD performs use extremely large number of calculations to simulate the behavior of fluids in complex environments and geometries. Within the computational region, CFD solves the Navier-Stokes equations (Figure 3) to obtain velocity, pressure, temperature and other quantities that may be required by a tackled problem. Recently CFD became a popular design and optimization tool with the help of commercially available software and advancing computer technology.

The CFD simulation problem called for assessment of liquid sulfur combustion inside the combusting chamber. The sulfur is atomized via spray nozzles in order for efficient burn off.

The commercially available CFD package ANSYS FLUENT (version 12.1) was used for the simulation of the sulfur combustion with air as an oxidizer. Air and combustion resulting gases inside the horizontal combustion chamber were set as primary phase flow (Eulerian approach). The primary phase used coupled models (momentum, turbulence, energy, species mixing and combustion) which required boundary conditions (BC's). Table 2 shows BC's for primary phase. This problem consisted of inlet BC and outlet BC, set as "mass flow rate inlet" and "constant pressure outlet" respectively. At the inlet mixture of gas with oxygen and nitrogen (air) was employed. These had

to be separate since oxygen was needed to the combustion process.

The sulfur injection was set as secondary phase (Lagrangian approach) where its inlet BC are based on spray injection parameters as determined empirically. The Lagrangian particles were set as "combusting." Table 3 shows injection BC of the injection nozzle. The Lagrangian particles were tracked using Discrete Phase Model (DPM). During computation, heat and mass transfer was coupled between primary and secondary phases.

To generate the computation domain (mesh) for the combustions chamber shown in Figure 5, Gambit (version 2.3.16) was utilized. The mesh consisted of 3,986,432 million of mixed cells. Due to its size and modeling complexity, the simulation required significant computer power and processing time.

The primary phase which consisted on gas mixture was mainly dependent on temperature as large temperature variations were expected. The gas was treated as "incompressible ideal gas" (no pressure variation, where operating pressure is used in ideal gas law), with physical properties such as density, heat capacity, viscosity, thermal conductivity and etc., set to be dependent on temperature. The operating pressure was set based on air inlet pressure (see Table 2).

The walls had a common (standard) setup, with no slip, adiabatic (insulated) and reflect for the combusting particles.

For combustion study, a species mixing model was used to accommodate combustion with oxygen from air. The evaporation and combustion of the liquid sulfur, using dispersed phase modeling capability was employed to compute coupled gas flow and liquid spray physics as aforementioned. The mixture fraction / PDF equilibrium chemistry model was used to predict the combustion of the vaporized fuel. This approach allows the simulation of combustion by solving a transport equation for a single conserved scalar, the mixture fraction. Property data for the species are accessed through a chemical database and interaction is modeled using a β-PDF.

The basis of the non-premixed modeling approach is that under a certain set of simplifying assumptions, the instantaneous thermochemical state of the fluid is related to a conserved scalar quantity known as the mixture fraction, f. The mixture fraction can be written in terms of the atomic mass fraction[8]

$$f = \frac{Z_i - Z_{i,ox}}{Z_{i,fuel} - Z_{i,ox}} \qquad (1)$$

where Z_i is the elemental mass fraction for element i. The ox and fuel refers to the values at the oxidizer and fuel stream inlet, respectively.

The β-PDF shape is given by equations 2-4, below.

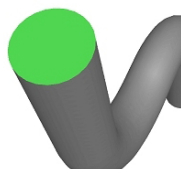$$p(f) = \frac{f^{\alpha-1}(1-f)^{\beta-1}}{\int f^{\alpha-1}(1-f)^{\beta-1}df} \qquad (2)$$

where

$$\alpha = \overline{f}\left[\frac{\overline{f}(1-\overline{f})}{\overline{f'^{2}}} - 1\right] \qquad (3)$$

$$\beta = (1-\overline{f})\left[\frac{\overline{f}(1-\overline{f})}{\overline{f'^{2}}} - 1\right] \qquad (4)$$

Radiation was modeled with the P-1 radiation model. This is a simplified radiation model that is based on the more general P-N model, which is based on the expansion of the radiation intensity I into an orthogonal series of spherical harmonics [8]. For combustion applications where the optical thickness is large, the P-1 model works reasonably well. In addition, the P-1 model can easily be applied to complicated geometries with curvilinear coordinates [8].

Continuous domain   **Discretized domain**

Equations applied to discretized domain

- ***Conservation of mass (Continuity)***

$$\frac{\partial \rho}{\partial t} + \nabla \cdot (\rho \vec{v}) = S_m$$

transient term   convective term   species variation term

- ***Momentum***

$$\frac{\partial}{\partial t}(\rho\vec{v}) + \nabla \cdot (\rho\vec{v}\vec{v}) = -\nabla p + \nabla \cdot (\overline{\overline{\tau}}) + \rho\vec{g} + \vec{F}$$

transient term   convective term   pressure drop   viscous term   gravity term   body forces

where $\overline{\overline{\tau}} = \mu\left[(\nabla\vec{v} + \nabla\vec{v}^{\,\mathrm{T}}) - \frac{2}{3}\nabla \cdot \vec{v}I\right]$

stress term components

- ***Energy***

$$\frac{\partial}{\partial t}(\rho E) + \nabla \cdot (\vec{v}(\rho E + p)) = \nabla \cdot \left(k_{\mathrm{eff}}\nabla T - \sum_j h_j \vec{J}_j + (\overline{\overline{\tau}}_{\mathrm{eff}} \cdot \vec{v})\right) + S_h$$

transient term   convective term   conduction term   diffusion term   viscous dissipation   chemical reactions and/or heat generation

where $E = h - \frac{p}{\rho} + \frac{v^2}{2}$

energy term components

Gradient of scalar: $\nabla p = \frac{\partial p}{\partial x}\vec{i} + \frac{\partial p}{\partial y}\vec{j} + \frac{\partial p}{\partial z}\vec{k}$

Gradient of vector: $\nabla(\vec{v}) = \left(\frac{\partial}{\partial x}\vec{i} + \frac{\partial}{\partial y}\vec{j} + \frac{\partial}{\partial z}\vec{k}\right)\left(v_x\vec{i} + v_y\vec{j} + v_z\vec{k}\right)$

Divergence of vector: $\nabla \cdot \vec{v} = \frac{\partial v_x}{\partial x} + \frac{\partial v_y}{\partial y} + \frac{\partial v_z}{\partial z}$
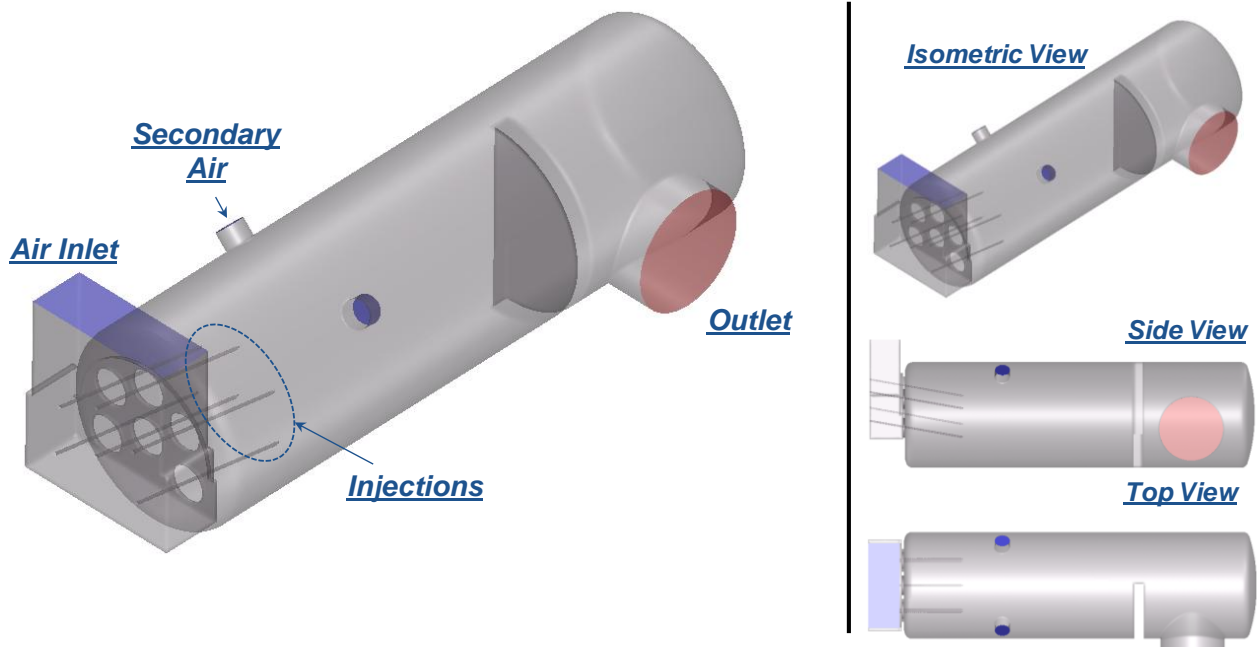
Figure 4 - **CFD Mesh and Governing Equations**

Figure 5 - **Sulfur Combustion Chamber**

	Units	Inlet	Outlet
Boundary condition	-	Mass flow	Const. pressure
Vol. flow rate	Nm^3/h	308,000	-
Mass flow rate	kg/s	113.9	-
Pressure	barg	0.569*	0**
Temperature	°C	122	1160***
Area	m^2	6.5	8.0
Avg. Velocity	m/s	19.67	126.8

*set as operating pressure, **set with respect to operating pressure, ***target temperature

Table 2. **Primary Phase Boundary Conditions**

	Units	Inlet
Total Vol. flow rate	m^3/h	29
Total Mass flow rate	kg/s	14.647
Pressure	barg	11
Temperature	°C	132
Number of injectors	-	5
Mass flow rate/inj.	kg/s	2.929
Injection velocity	m/s	35
D minimum ($D_{V0.01}$)	μm	37
D mean ($D_{V0.50}$)	μm	505
D maximum ($D_{V0.99}$)	μm	1087
Spraed Parameter (RRD)	-	3.0

Table 3. **Injection Boundary Conditions**

RESULTS (Experimental & Numerical)
Experimental Results

The results of the PDI measurements provide a representative characterization of the atomizer effectiveness at the 36" downstream investigation location. As outlined and described in the above sections, the results from testing are provided in Table 3. The Sauter Mean Diameter (D_{32}) as well as other representative diameter statistics based on the volume flow is presented. These results allow the evaluation, qualitatively, of the dependence of drop size on the liquid flow rate and pressure.

Mean diameters and distribution parameters			
Arithmetic mean (D_{10}):	233 μm	Volume median diameter ($D_{V0.5}$) :	505 μm
Surface mean (D_{20}):	277 μm	Number median diameter ($D_{N0.5}$) :	187 μm
Volume mean (D_{30}):	320 μm	$D_{V0.1}$:	270 μm
Surface-diameter mean (D_{21}):	330 μm	$D_{V0.9}$:	754 μm
Evaporative mean (D_{31}):	375 μm		
Sauter mean (D_{32}):	427 μm	Relative span factor (RSF) :	0.96
Herdan mean (D_{43}):	509 μm	Coefficient of variance (CV) :	2.7

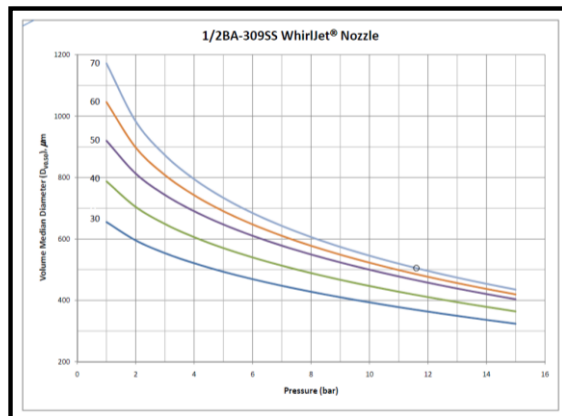Table 3. **1/2BA-309SS70 Injector Characterization**

Figure 6 **Spray Characterization Results**

With an increase in liquid feed pressure:
- there is a decrease in median drop size,
- and there is an increase in mean drop velocity.

CFD Results

The CFD results provide great insight into the mixing mechanisms and spray interactions in complex environments such as combustion. The boundary conditions, as described above, mimic the intended real world operation of this sulfur feed injection nozzle and provided quality inputs for numerical analyses. These CFD calculations, based on the k-epsilon turbulence model, were allowed to run through hundreds of iterations until a steady-state solution was realized. This solution was deemed acceptable when the calculation residuals (changes in the results from one iteration to the next) were negligibly low and good convergence was achieved. Figure 7 provides the results of the path lines of the gas flow traced through the combustion chamber. This provides a preliminary assessment of injection locations. Due to the relative momentum of the gas stream, droplet trajectories and particle tracks will be influenced. At the six entry points of air into the chamber an increased velocity profile can be seen. This will affect the droplets, pulling drops towards the base of the combustion chamber. If this effect is large, there is potential for wall impingement, resulting in wall damage and reduced efficiency of the process.
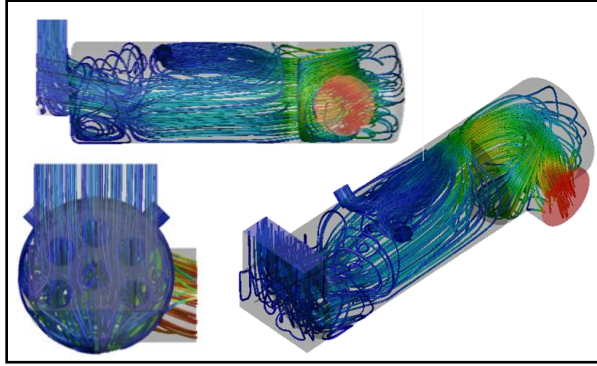
Figure 7 **Gas Path Lines Through Combustion Chamber**

Additionally, the effects of the secondary air on the general flow can be assessed. The secondary air has a significant affect on the top 1-3 injected sprays. There is poor distribution of this secondary air through the combustion chamber.

The velocity profile demonstrates the high velocity magnitude of both fluids as they enter the mixing / combustion region. As would be expected, there are very low velocity regions in the combustion chamber near the walls and the mixed flow has a fairly uniform, mid-level velocity profile as it moves through the primary combustion area (see figure 7).

The combustion was considered through with a non-premixed modeling approach. The property data for the species were accessed through a chemical database and the interaction was modeled using a β-PDF. The results of the combustion based on species contents are shown in figure 8-9.

The primary focus of this study was to verify that the sulfur injection droplets were fully devolatilized prior to the exit of the combustion chamber. Failure in this endeavor could lead to downstream damage and increased cost of operations. From figure 8, it is evident that the sulfur combustion is complete prior to the baffle wall. From the injection planes (the right side of figure 9), it is evident that the oxygen from the secondary air results in greater combustion rates at the top of the combustion chamber as compared to the lower regions of the combustion chamber. This trend is mirrored in figure 9, with the examination of the oxygen profiles within the combustion chamber.
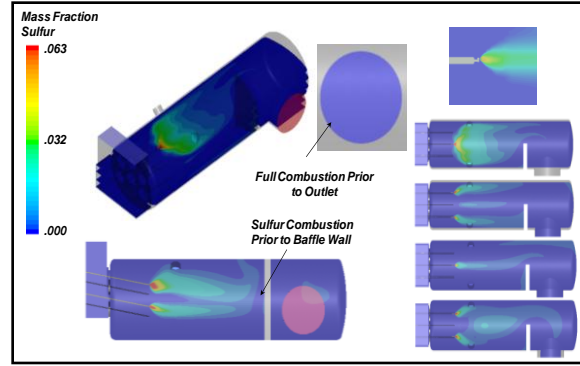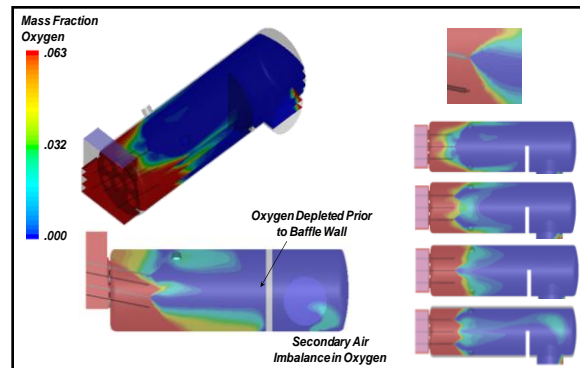

Figure 8 - **Mass Fraction of Sulfur**

Figure 9 - **Mass Fraction of Oxygen**

The combustion of the sulfur injections can also be examined through visualizing the spray emitted from the injectors. An initial DPM Concentration (DPMC) value was used to define Spray Plume Boundary (SPB) and visualize the spray region as shown in Figure 8. The iso-surface of DPMC was based on matching peaks of CFD DPMC value and experimental volume flux at measured with the PDI. To obtain cut-off DPMC, the cut-off volume flux point at about 0.002 $cm^3/cm^2/s$ was matched with 0.001 kg/m^3.

There is some potential for droplet impingement with the base of the spray chamber (this region is highlighted in red). From the top view (shown on the left side of figure 10), there is no evidence of wall impingement along the sides of the combustion chamber however the full diameter of the combustion chamber is utilized with sulfur spray. This would indicate that the spray angle of the injector is optimal for the application.
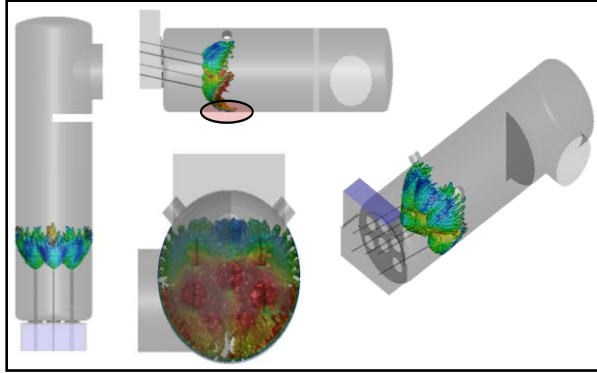
Figure 10 **Spray Visualization**

Based on the inlet gas velocity contours the injection angle was determined. Alternate injection angles from 0 - 20° off the horizon were examined. The results of these preliminary simulations are shown in figure 11. These simulations were not run to full convergence and thus are for reference only. The results demonstrate the importance of proper injector design for optimal combustion with minimal wall impingement. The even with horizon injectors indicate no wall impingement on the base of the combustion chamber, however there is some negative interaction with the secondary air inlet. The result is some potential for impingement on the top of the chamber and, more importantly, less desirable combustion rates. In order for evaporation to occur, the oxygenated gas must mix with the distributed sulfur droplets. This increased surface area contact allows the reaction to occur more quickly.
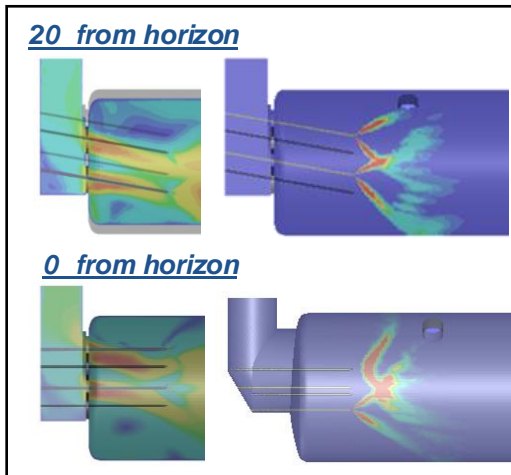

Figure 31 **- Injection Angle Evaluation**

The resulting temperature profiles for the combustion chamber were examined. The temperature profiles are displayed in Figure 12. Temperatures were not uniform from top to bottom. This is primarily due to the fact that the secondary air adds cooler air and also acts as an additional source of oxygen to improve the combustion. The rate of combustion is slightly higher towards the top of the combustion chamber.

Temperatures at the outlet were found to be around 1400°C. This is slightly above the measured values collected from practice of 1100-1200°C. This error could be improved with a more complex combustion model and more complex radiation model. However the simulation does prove to be a reasonable assessment of the sulfur combustion application.
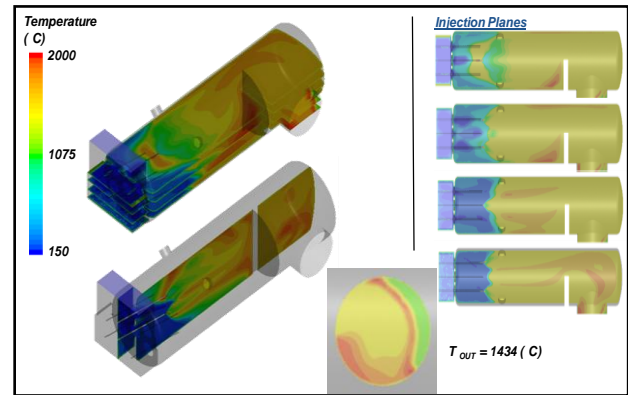

Figure 4 **Temperature Profiles in the Combustion Chamber**

DISCUSSION AND CONCLUSIONS
Engineering optimization of injectors

The optimal nozzle design for sulfur feed injection for this combustion application incorporates the Spraying Systems Co. patented nozzle optimized based on the testing results presented in this report. The Spraying Systems Co. nozzle can provide the necessary spray characteristics with minimal wall impingement and full combustion of injected sulfur. Drop sizes ranging from less than 37μm to greater than 1087μm were created at the selected operating conditions.

The results of the CFD analyses provide insight into the internal mixing mechanics of the sulfur combustion process and allow for better optimization. By performing high-accuracy, steady-state simulations of the nozzle a better understanding of the governing mixing forces and their relative effect on the internal mixing and combustion is evident. It is clear from these models, see Figures 7-11, that the injected molten sulfur will thoroughly combust, without interactions leading to increased operation costs or equipment damage.

The in-depth analyses of these, and previous, tests provide experimental, computational, and analytical basis for the optimization parameters which are employed in the use of this sulfur combustion injector. With improved knowledge of the internal mechanics and the external spray pattern, optimization of the noz-

zle at these operating conditions can be done very effectively.

REFERENCES

1. Lefebvre, A.W., Atomization and Sprays, Hemisphere Publishing Corporation,1989, p.1-78.
2. Bachalo, W.D., "Experimental Methods in Multiphase Flows", International Journal on Multiphase Flow, Vol.20,Suppl. pp.261-295, 1994
3. Bachalo, W.D., "A Method for Measuring the Size and Velocity of Spheres", by Dual Beam Light Scatter Interferometry, Applied Optics, Vol. 19, No. 3, February 1, 1980.
4. Bachalo, W.D. and Houser, M.J., "Spray Drop Size and Velocity Measurements Using the Phase/Doppler Particle Analyzer", Proceedings of the International Conference on Liquid Atomization and Spray Systems (Third International), July, 1985.
5. W. D. Bachalo and M. J. Houser, "Phase Doppler Spray Analyzer for Simultaneous Measurement of Drop Size and Velocity Distribution", Optical Engineering, Vol. 23, No. 4, pp. 583, 1984.
6. R. J. Schick, "A Guide to Drop Size for Engineers," Spraying Systems Co. Bulletin 459.
7. Properties of Sulphur, Sulphuric-Acid.com, May 2005.
8. ANSYS *Fluent Theory Guide*, Release 13.0, November 2010.
9. Fluent Inc. *FLUENT 6.3 User's Guide*, 2000.